energies

MDPI

Review

A Review of the Parameters Affecting a Heat Pipe Thermal Management System for Lithium-Ion Batteries

Kittinan Boonma [1], Napol Patimaporntap [1], Hussein Mbulu [1], Piyatida Trinuruk [1], Kitchanon Ruangjirakit [1], Yossapong Laoonual [1] and Somchai Wongwises [1,2,*]

[1] Fluid Mechanics, Thermal Engineering and Multiphase Flow Research Lab (FUTURE), Department of Mechanical Engineering, Faculty of Engineering, King Mongkut's University of Technology Thonburi (KMUTT), Bangmod, Bangkok 10140, Thailand
[2] National Science and Technology Development Agency (NSTDA), Pathum Thani 12120, Thailand
* Correspondence: somchai.won@kmutt.ac.th; Tel.: +66-24709115

Abstract: The thermal management system of batteries plays a significant role in the operation of electric vehicles (EVs). The purpose of this study is to survey various parameters enhancing the performance of a heat pipe-based battery thermal management system (HP-BTMS) for cooling the lithium-ion batteries (LIBs), including the ambient temperature, coolant temperature, coolant flow rate, heat generation rate, start-up time, inclination angle of the heat pipe, and length of the condenser/evaporator section. This review provides knowledge on the HP-BTMS that can guarantee achievement of the optimum performance of an EV LIB at a high charge/discharge rate.

Keywords: battery thermal management; heat pipe; lithium-ion battery; electric vehicle; thermal performance

Citation: Boonma, K.; Patimaporntap, N.; Mbulu, H.; Trinuruk, P.; Ruangjirakit, K.; Laoonual, Y.; Wongwises, S. A Review of the Parameters Affecting a Heat Pipe Thermal Management System for Lithium-Ion Batteries. *Energies* **2022**, *15*, 8534. https://doi.org/10.3390/en15228534

Academic Editors: Marco Marengo and Noradin Ghadimi

Received: 7 August 2022
Accepted: 30 October 2022
Published: 15 November 2022

1. Introduction

Air pollution is a result of the heavy traffic of internal combustion engine vehicles. Electric vehicles (EVs) do not emit air pollution during operation and are one of the alternative modes of transportation that help reduce air pollution.

In EVs, the battery is the main power source. Lithium-ion is one of the key components in EV batteries. The advantages of these batteries are that they have high energy density, high power density, lighter weight, better recyclability, and a long life-cycle compared to other types of batteries [1–5]. Furthermore, they have no effect on memory [1,2,4,5]. However, the main problem with lithium-ion batteries (LIBs) is the temperature increase during the charge/discharge process. Therefore, an appropriate battery thermal management system (BTMS) must be provided to maintain a uniform temperature distribution and optimal temperature range in an EV battery.

Normally, the maximum temperature (T_{max}) and temperature difference (ΔT) on the battery surface increase due to the heat generation in a LIB. The heat generated during battery operation originates from reversible and irreversible heat sources. The former includes entropy changes during electrochemical reactions. The latter includes internal resistance, concentration, activation, and ohmic polarization [6].

The accumulation of heat accelerates aging and shortens the battery's life span, leading to a lower charge/discharge efficiency and reduced battery performance. Extremely high temperatures can lead to thermal runaway [7]. Inversely, low temperatures can result in a higher internal resistance, which also reduces battery performance [8]. Therefore, a battery should be operated under an optimal temperature range. The optimum maximum temperature (T_{max}) for LIBs is 25–40 °C [9–11], and the temperature difference (ΔT) of the batteries must be maintained at below 5 °C [9–12].

A well-designed BTMS is necessary to ensure that batteries are working in suitable operating conditions [13]. In the design of a BTMS, safety, ease of maintenance, size, weight,

and potential applications have to be taken into account [14]. BTMSs have been categorized into four main groups: air cooling, liquid cooling, phase change material cooling, and heat pipe cooling, as shown in Figure 1.

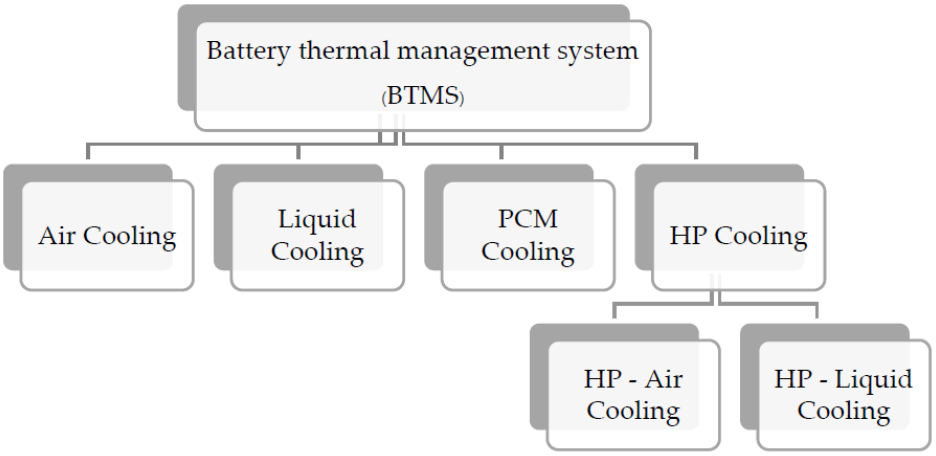

Figure 1. Classification of battery cooling systems.

Air cooling BTMSs are used mainly because they have uncomplicated structures and are inexpensive and lightweight. However, despite their advantages, air cooling BTMSs fail severely in stressful conditions such as in high ambient temperatures and high charge/discharge rates, leading to uneven temperature distributions and high temperature differences [15–18]. Researchers have tried to improve the performance of air cooling BTMSs by considering structural designs, battery layout optimization, and control strategies, including the use of forced convection systems [17,19,20].

Due to their high heat transfer coefficients, liquid cooling BTMSs are more efficient for LIBs [21]. They can be divided into two types—direct and indirect contacts [22]—corresponding to whether the liquid is in direct contact with the battery. However, if an EV is involved in an accident, the possibility of the liquid leaking into the battery is high [23], resulting in the short circuiting of the battery pack.

Phase change materials (PCMs) also can be used in BTMSs and work well for maintaining temperature uniformity in a battery module/pack [24]. However, a drawback is that PCMs have low thermal conductivity [25]. Researchers have proposed various methods for enhancing PCMS's heat transfer capacities, such as adding fins [26], metal mesh [27], graphite [28], or metal foam [24]. When a PCM absorbs high heat from a battery surface, the PCM melts and its volume expands; therefore, a leak-proof design is needed [21].

The application of a heat pipe for cooling is an emergent passive cooling technique. Heat pipes are often called superconductors of heat due to their heat transfer rates and minimal heat loss. A heat pipe consists of a condenser section, an adiabatic section, and an evaporator section, as shown in Figure 2. Liquid in the evaporator section absorbs heat and vaporizes. The vapor then flows to the condenser section, where it condenses. The condensed liquid then returns to the evaporator section thought either capillary force, centrifugal force, or gravitational force, and it re-vaporizes to repeat the cycle [29]. Heat pipes have been widely used in cooling applications where their evaporator sections are attached to heat sources.

A heat pipe-based battery thermal management system (HP-BTMS) is one of the technologies that meets almost all the required conditions for a BTMS, ensuring that the battery operates at an optimal temperature. The advantages of such a system are its high heat transfer rate, low weight, compact size, low cost, long life, and high capacity for moving heat from the inside of the battery pack to the outside [30]. Moreover, the heat pipe structure in the condenser section can be coupled with forced air [31] or a water spray [32] to ensure maximum performance. Some investigators have coupled an aluminum fin to the condenser to enhance the heat transfer rate [33]. However, with an HP-BTMS, a problem

still exists with keeping the battery temperature within the optimum range, especially when the charge/discharge rate is high. Some researchers have used plate flat heat pipes for BTMSs to obtain temperature uniformity of the battery pack [34–36].

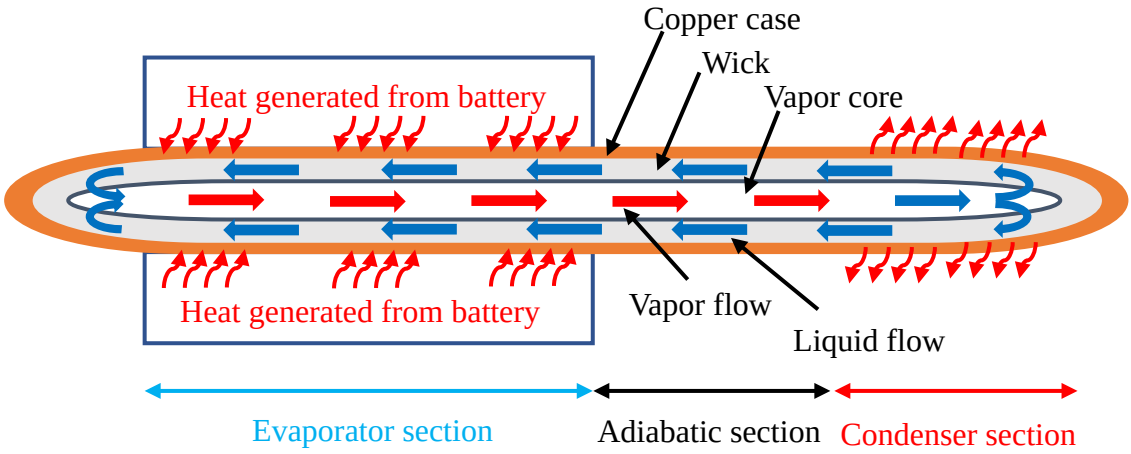

Figure 2. Schematic diagram of a heat pipe.

To solve this problem, a PCM is used in conjunction with a heat pipe to reduce the temperature difference and maximum temperature [37]. In addition, the thermal behaviour of a constructal theory-based heat pipe was studied by Boonma et al. [38]. The results of their study provided information on adaptable thermal management systems for the development of compact battery packs. By increasing the condensing areas of heat pipes, the size and number of heat pipes needed for cooling could be reduced.

Table 1 summarizes some related research on heat pipes, categorized as air cooling and liquid cooling depending on the coolant used in the condenser end. These previous studies show that a large number of researchers have investigated the effects of the variables related to the thermal performance of HP-BTMSs. Nevertheless, no review paper has put all of that information together. Thus, the objective of this paper is to report the effects of the relevant parameters (heat generation rate, ambient temperature, coolant temperature, coolant mass flow rate/air velocity, condenser/evaporator section length, inclination angle, and start-up time) on the performance of HP-BTMSs.

Table 1. Summary of the heat pipe cooling systems reported in the literature.

Fluid Used for Cooling at Condenser End	Authors	Heat Source	Heat Pipe	Heat Generation Rate	T_{amb}	Coolant Inlet Temp.	T_{max}	ΔT
Water	Mbulu et al. [5] (Experiment)	Battery surrogate	16 heat pipes (copper)	30–60 W	-	30 °C	<55 °C	<5 °C
Water	Liang et al. [39] (Experiment)	2 simulated batteries (battery surrogate)	4 heat pipes (copper)	20–50 W	15–35 °C	15–35 °C	<40 °C	<5 °C
Air and water	Nasir et al. [40] (Experiment)	Proxy cells (battery surrogate)	2 heat pipes (aluminium plate)	10–35 W	-	-	<50 °C	<5 °C
Water	Gan et al. [41] (Experiment)	24 cylindrical cells	15 heat pipes (copper)	1 and 2 C discharge	25 °C	20 °C	<40 °C	<5 °C
Natural convection	Zhang and Wei [42] (Experiment)	5 prismatic cells (16 V, 8.5 Ah)	6 flat heat pipes (aluminium plate)	4, 6, and 8 C rate	25 °C	-	<40 °C	<5 °C

2. Parameters Affecting the Performance of a HP-BTMS

2.1. Effects of the Heat Generation Rate

Heat generation from batteries is unavoidable. Therefore, the BTMS design is essential to keep the battery temperature within the proper values.

The heat generated is related to the high current rate (C rate) or the charge/discharge rate. The total heat generated ($\dot{Q}_{total}$) is calculated as [6]:

$$\dot{Q}total = \dot{Q}rev + \dot{Q}irr = -I{\cdot}T\,\frac{dU_{OC}}{dT} + I^2{\cdot}R, \quad (1)$$

where I, T, $\frac{dU_{OC}}{dT}$, and R are the current, temperature, entropy coefficient, and internal resistance of the cell, respectively.

Hu et al. [6] measured the heat generation of LIBs during operation to analyze the BTMS. Their tests on the effects of C rates on heat generation were performed at T_{amb} = 25 °C. The C rate values considered for charging/discharging were C/3, 0.5 C, 1 C, 2 C, 3 C, and 4 C, as shown in Figure 3.

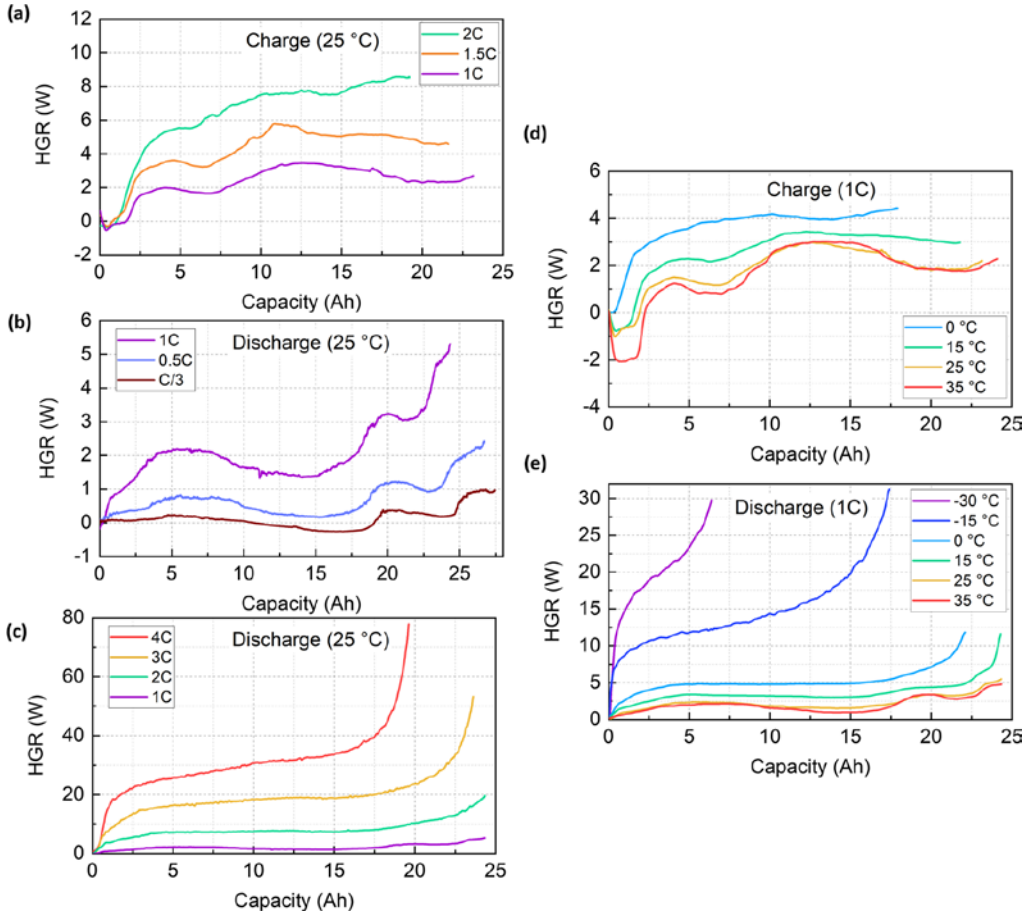

Figure 3. Measurement results of heat generation rates at different C rates during (**a**) charging rates of 1 C, 1.5 C, and 2 C at T_{amb} 25 °C; (**b**) discharging rates of C/3, 0.5 C, and 1 C at T_{amb} 25 °C; (**c**) discharging rates of 1 C, 2 C, 3 C, and 4 C at T_{amb} 25 °C; (**d**) charging rate of 1 C at T_{ambs} of 0 °C, 15 °C, 25 °C, and 35 °C; and (**e**) discharging rate of 1 C at T_{ambs} of −30 °C, −15 °C, 0 °C, 15 °C, 25 °C, and 35 °C (from Hu et al. [6], with permission from Elsevier).

Zeng et al. [43] applied a hybrid micro heat pipe array (MHPA) to the BTMS of cylindrical batteries. Compared to a system without the MHPA, for a 1 C discharging

process, the T_{max} was reduced by 34.11% and the ΔT decreased from 3.66 to 0.66 °C. For the 3 C discharging process, the T_{max} and ΔT decreased to 41.03 and 2.16 °C, respectively.

Some researchers have used a battery surrogate to represent a real battery. The heat input power (Q) is analogous to the heat generated by an actual LIB during acceleration and high charging or discharging conditions. The heat generated might range from 10 to 40 W under normal working conditions. In contrast, in severe working conditions, it might range from 50 to 70 W. Normally, when the heat generated, T_{max}, and ΔT increase, the extensive heat produced can affect the LIB severely to the point where it is beyond recovery. Therefore, the heat transfer rate (Q_{HP}) of a heat pipe depends on the input power (Q), which can be calculated as [44]:

$$Q_{HP} = Q - \frac{(T_{sat,e} - T_{sat,c})kA_k}{L_{ce}}, \quad (2)$$

where $T_{sat,e}$ and $T_{sat,c}$ are the evaporator and condenser saturation temperatures, respectively. The variables k and A_k are the heat pipe's thermal conductivity and the cross-section area of the heat pipe, respectively, and L_{ce} is the length between the points where the $T_{sat,e}$ and $T_{sat,c}$ are measured. Equation (2) shows that when the input power (Q) increases, the Q_{HP} increases and, therefore, the battery surface temperature (T_H) increases, which leads to an increase in T_{max} and ΔT.

Rao et al. [45] conducted an experiment to investigate the temperature distribution of a battery when the input power varied from 10 to 60 W. The results showed that the T_{max} could be kept below 50 °C when the heat generation rate was below 50 W and the ΔT was less than 5 °C when the heat generation rate was 30 W or less.

Wang et al. [46] investigated the effectiveness of heat pipes by constructing a simulated heat source in the range of 2.5 to 40 W/cell. They found that the heat pipe could regulate the temperature of a battery to below 40 °C when the heat generated by the battery was less than 10 W/cell. Additionally, the analysis showed that even when the battery generated heat in the range of 20–50 W/cell, which was considered thermal abuse, the heat pipe could keep the temperature of the battery below 70 °C, preventing thermal runaway.

Mbulu et al. [5] reported that their HP-BTMS with sandwiched L- and I-shaped heat pipes was able to keep a battery's temperature under 55 °C, even when the heat produced from the battery was 60 W. When the heat input increased to 30, 40, 50, and 60 W, the T_{max} on the battery surface was 43.82, 46.59, 50.96, and 54.38 °C, respectively, as shown in Figure 4.

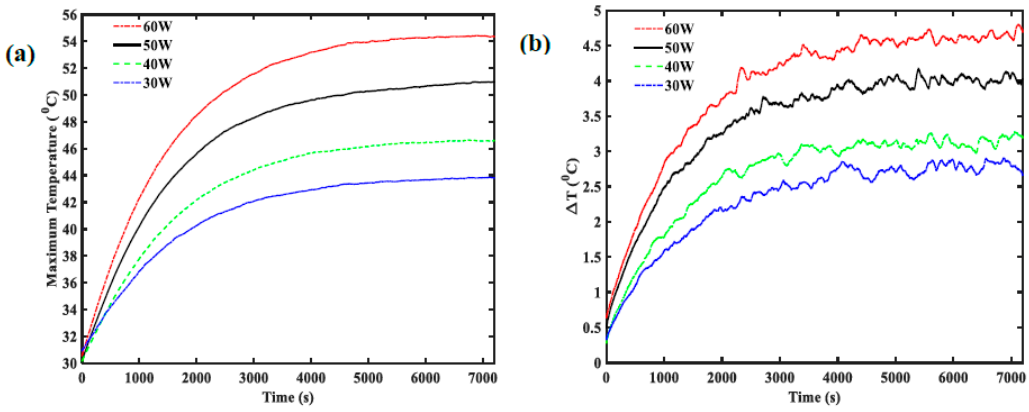

Figure 4. The variation of (**a**) T_{max} and (**b**) ΔT at different input powers and a mass flow rate of 0.0167 kg/s (from Mbulu et al. [5], with permission from Elsevier).

According to the information gathered above, the heat generation rate of a battery is the result of the current rate or heat input, which affects the T_{max}, ΔT, and battery performance. This could lead to an internal short circuit and thermal runaway [47]. Therefore, it is important to consider heat generation and the related parameters when designing an

HP-BTMS. Table 2 summarizes investigations of the heat pipe cooling system at different heat generation rates.

Table 2. Summary of studies of the heat pipe cooling system at different heat generation rates and coolant temperatures.

Fluid Used for Cooling at Condenser End	Authors	Heat Source	Heat Pipe	Heat Generation Rate	T_{amb}	Coolant Flow Rate	Coolant Inlet Temp.	T_{max}	ΔT
Water	Mbulu et al. [5] (Experiment)	Battery surrogate	16 heat pipes (copper)	30–60 W	-	1 LPM	30 °C	<55 °C	<5 °C
Water	Rao et al. [45] (Experiment)	Aluminium rectangular heater (battery surrogate)	4 heat pipes (copper)	10–60 W	-	-	25 ± 0.5 °C	<50 °C	<5 °C
Water	Liang et al. [39] (Experiment)	Simulated battery (battery surrogate)	4 heat pipes (copper)	20–50 W	15, 25, 30, and 35 °C	1, 2, and 3 LPM	15–35 °C	<40 °C	<5 °C
Air	Yao et al. [48] (Experiment)	Heater (battery surrogate)	MHPA	10–50 W	24.8 °C	3.3 ms^{-1}	24.8 °C	<40 °C	3.44 °C
Air	Zhang and Wei [42] (Experiment and simulation)	5 prismatic cells (3.65 V, 8.5 Ah)	6 flat heat pipes (aluminium)	2, 4, 6, and 8 C rate	25 ± 2 °C	-	25 ± 2 °C	<40 °C	<5 °C
Water	Wang et al. [49] (Experiment and simulation)	12 cylindrical cells (3.7 V, 1.96 Ah)	5 heat pipes (copper)	3 and 5 C discharge	25 °C	2 LPM	25 °C	27.62 °C	1.08 °C
TiO_2 nano-fluid	Chen and Li [50] (Experiment)	Prismatic cells (3.2 V, 68 Ah)	PHP	0.5, 1, and 1.5 C discharge	25, 30, and 35 °C	-	25 °C	<42.22 °C	<2 °C
Water and refrigerant	Jouhara et al. [51] (Experiment)	16 prismatic cells (2.3 V, 23 Ah)	Flat heat pipe (heat mat)	4 C	-	9.5 LPM	-	<28 °C	±1 °C

2.2. *Effects of the Ambient Temperature*

The ambient temperature is a factor that contributes to either a decrease or increase of the temperature surrounding the LIB's position. The ambient temperature (T_{amb}) contributes to an increase in the LIB's heat generation rate if the T_{amb} is above 15 °C. However, when the T_{amb} is below 15 °C, the chemical reaction will be impeded; thus, the output power generated will deteriorate [39]. The increased heat generation rate results in increases in the T_{max} and ΔT.

Behi et al. [52] carried out an experimental study to analyze the impact of the T_{amb} of the air on a battery module's temperature distribution, as shown in Figure 5. The researchers investigated three ambient temperatures: 10, 26, and 35 °C. The experiment clearly proved that the T_{amb} of the air has a critical effect on the temperature distribution of a battery. When the T_{amb} is low, the temperature distribution on the battery surface decreases.

Alihosseini and Shafaee [53] analyzed a battery's thermal performance based on winter and summer temperatures of 18, 28, and 33 °C, as shown in Figure 6. In this experiment, the T_{amb} was adjusted and controlled in a test chamber. Li et al. [54] studied the effects of the T_{amb} on the T_{max} and ΔT. They found that a high T_{amb} will cause the T_{max} to rise above the optimal temperature and cause the HP-BTMS's thermal performance to decrease. Meanwhile, the ΔT of the battery decreases when the T_{amb} increases. This result implies that a low T_{amb} will elevate the ΔT.

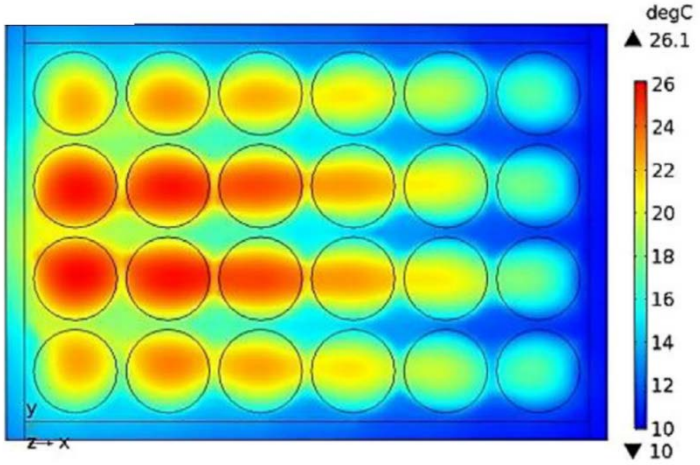

(**a**)

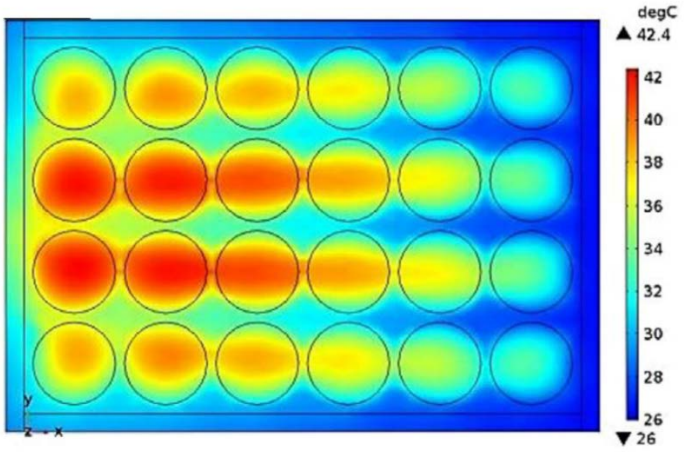

(**b**)

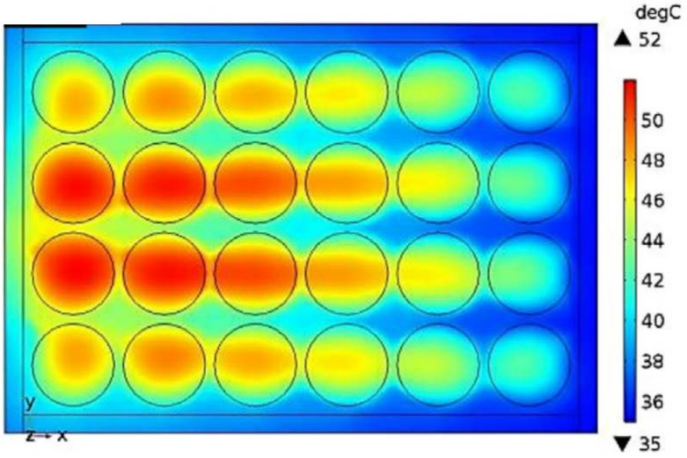

(**c**)

Figure 5. Battery surface temperatures at T_{amb} of (**a**) 10 °C, (**b**) 26 °C, and (**c**) 35 °C (from Behi et al. [52], with permission from Elsevier).

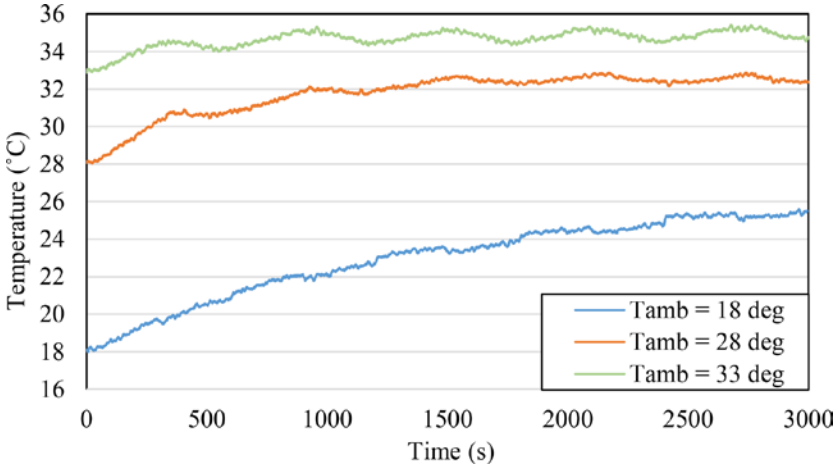

Figure 6. Variation in battery surface temperatures with different ambient temperatures (from Alihosseini and Shafaee [53], with permission from Elsevier).

After reviewing the literature on the ambient temperature's effects on heat pipe performance, we concluded that an HP-BTMS should be operated in a suitable environment to achieve optimal thermal performance for the LIB.

2.3. Effects of the Coolant Temperature

To keep the temperature of the battery within the optimal range, the coolant T_{max} must be controlled. A low coolant temperature results in a decrease in the maximum temperature. Too low of a coolant temperature results in a high temperature difference, which leads to a reduction in battery capacity. Therefore, it is necessary to use the optimum coolant temperature.

Ye et al. [10] studied the effects of coolant temperature at a fixed flow rate. They chose coolant temperature values of 15, 20, and 25 °C and found that with a battery heating load of 100 W, the temperature could be kept below 40 °C if a coolant temperature of 15 °C was used. Additionally, they also discovered that although the use of a low coolant temperature increased thermal performance, if the temperature was too low, it led to a significant increase in ΔT.

Liang et al. [39] analyzed the effects of coolant temperature on the T_{max} and ΔT of a battery at ambient temperatures of 25 and 35 °C. A lower coolant temperature lowered the T_{max}. In this study, the T_{max} of the battery was found to be above 40 °C when the coolant temperature was approximately 20 °C. On the other hand, if the coolant temperature was reduced too much, the temperature was more unevenly distributed, as shown in Figure 7.

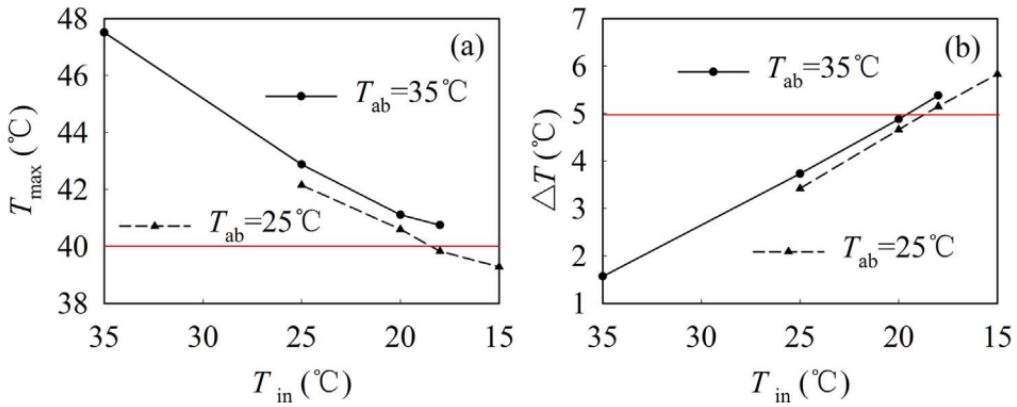

Figure 7. (**a**) T_{max} and (**b**) ΔT of a battery under different inlet coolant temperatures with an input power of 40 W and flow rate of 2 LPM (from Liang et al. [39], with permission from Elsevier).

Li et al. [54] investigated the effects of coolant temperature on battery cooling capacity under an ambient temperature of 40 °C. The study was conducted using batteries with a discharge rate of 4 C. The results showed that the battery temperature could be kept below 40 °C when the coolant temperature was 20 °C, as shown in Figure 8.

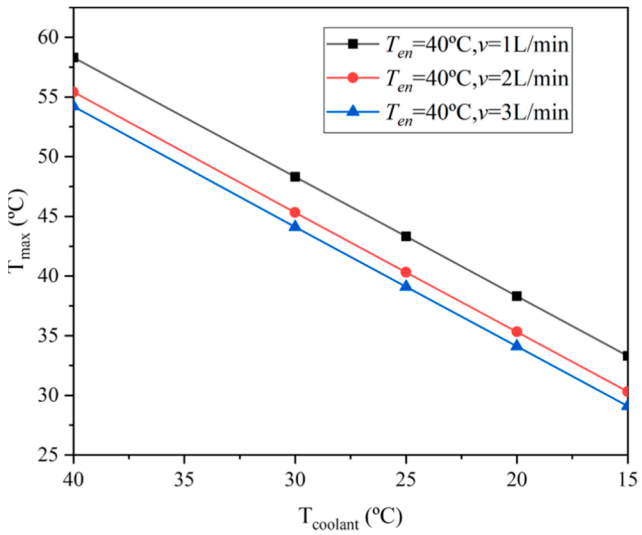

Figure 8. Variation of T_{max} at a 4 C discharge rate with different coolant temperatures (from Li et al. [54], with permission from Elsevier).

Based on the above studies on the effects of coolant temperature, we concluded that reducing coolant temperature is one method for improving the performance of an HP-BTMS. However, the disadvantage is that if the coolant temperature is reduced too much, the temperature of the battery surface will be unevenly distributed. Therefore, the coolant temperature should be within the appropriate range.

2.4. Effects of the Coolant Flow Rate

The mass flow rates of the coolant in the condenser can affect the T_{max} and ΔT. When the coolant mass flow rates increase, the T_{max} and ΔT decrease. Nevertheless, when the mass flow rates increase beyond the optimal value, it has no significant impact on either the T_{max} or ΔT.

Researchers have also found that pressure loss in the cooling channel significantly increases as the coolant mass flow rate increases, which signifies that only increasing the flow rate of the coolant is not applicable for enhancing the performance of an HP-BTMS [39,40,55].

Ye et al. [10] investigated the mass flow rate's effects on the T_{max} and ΔT. They found that the T_{max} and ΔT decreased greatly when the flow rate increased from 1 to 2 LPM. However, when the flow rate increased from 2 to 3 LPM, the T_{max} and ΔT decreased only slightly.

Wu et al. [56] investigated the effects of air velocities between 0 and 3 ms^{-1} with a battery discharge rate of 5 C, as shown in Figure 9. They found that the T_{max} decreased with the rising air velocity. However, when the air velocity increased further, the T_{max} decreased at a lower rate due to the limitation of the phase transition process.

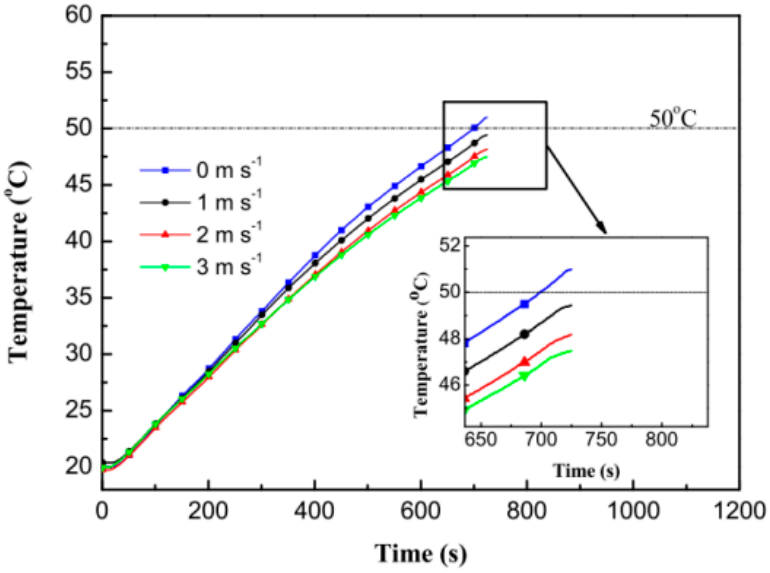

Figure 9. Transient temperatures under different air velocities at a 5 C discharge rate (from Wu et al. [56], with permission from Elsevier).

Wan [57] found that an increase in the coolant flow rate from 0.5 to 2 LPM resulted in a decrease in the T_{max} of approximately 8.9 °C (16.9%). In addition, when the coolant flow rate increased from 2 to 8 LPM, the T_{max} decreased by approximately 4.07 °C (approximately 9.3%). It should be noted that when the coolant flow rate increased from 0.5 to 8 LPM, the pressure drop (ΔP) increased remarkably from 1.35 Pa to 77.76 Pa, as shown in Figure 10.

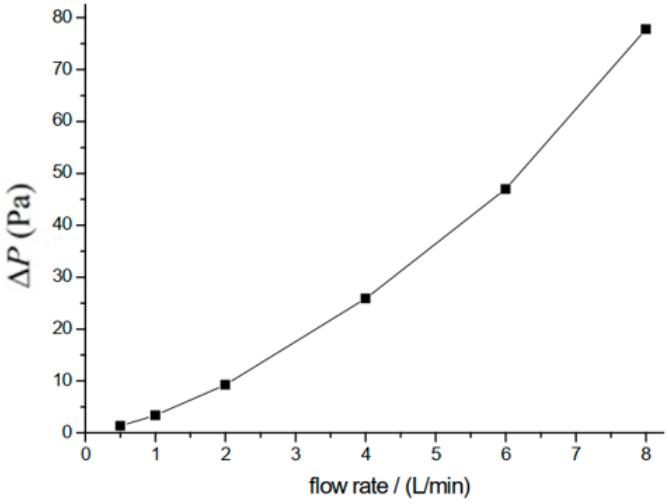

Figure 10. Effects of coolant flow rates on pressure drops [57].

Gan et al. [41] confirmed the effects of the coolant's mass flow rates on drops in pressure. An increase in the coolant flow rate resulted in an increased pressure drop in the coolant circulation loop system. The authors found that when the coolant mass flow rate increased from 0.5 to 2 LPM, the pressure drop increased from 872.5 to 7995.3 Pa, as shown in Figure 11. The authors suggested the optimum flow rate in their study was 0.5 LPM because this flow rate provided a relatively low pressure drop.

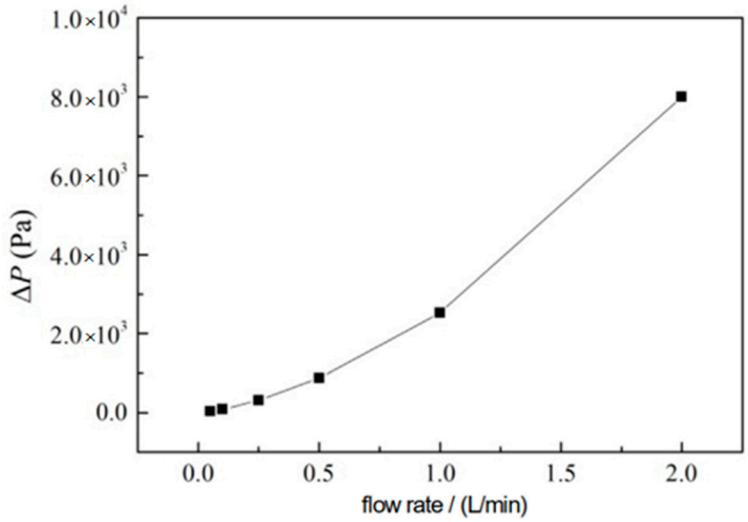

Figure 11. Effects of coolant flow rates on pressure drops (Pa) (from Gan et al. [41], with permission from Elsevier).

Yao et al. [48] investigated the performance of heat pipes at air velocities ranging from 0 to 3.5 ms^{-1} with a heat generation rate of 40 W. They found that at an air velocity of 3.5 ms^{-1}, the battery temperature could be maintained at 40 °C, and at an air velocity of 0 ms^{-1} (natural cooling), the battery temperature was 75 °C. They also found that at air velocities of between 2.5 and 3.5 ms^{-1}, there were decreases in temperature. However, the rate of the temperature drop was noticeably reduced. In terms of the temperature difference, the mean value for all air velocities applied was 2 °C. Therefore, they concluded that the air velocity had no pronounced effect on the temperature distribution.

Wan [58] investigated the effects of coolant flow rates of between 1 and 3 LPM on the cooling performance of an HP-BTMS. Both the T_{max} and ΔT were reduced as the coolant flow rate decreased. Nevertheless, for coolant flow rates ranging from 2 to 3 LPM, the T_{max} and ΔT decreased to lesser extents.

Concerning the coolant flow rate's effects, many researchers have found that increasing the coolant flow rate is a way to increase the thermal performance of an HP-BTMS. However, using a very high coolant flow rate is not necessary because at a very high coolant flow rate, the battery temperature changes very little. In addition, to achieve a higher coolant flow rate, more energy is needed to deliver the fluid. Therefore, an appropriate coolant flow rate is needed to increase the thermal performance of an HP-BTMS.

Furthermore, researchers have studied the effects of the mass flow rate on the heat pipe's thermal resistance and found that an increase in the mass flow rate led to a decrease in the heat pipe's thermal resistance [40]. The main cause of this was the increase in heat transfer dissipation caused by the increased water motion [40].

2.5. Effects of the Start-Up Time

The start-up time is the time that a BTMS takes to start after the battery is initiated. It is not worth allowing the BTMS to cool the battery immediately after it starts up because the heat has not yet accumulated in the battery. Synchronized cooling, in which the BTMS works immediately, should not be used due to the overcooling of the battery [39]. This overcooling decreases the Li-ion diffusivity and the rate of the chemical reaction under a low T_{amb}, which results in a higher over-potential and a lower charge (discharge) capacity [39].

To start a BTMS, one should allow the battery to run and heat up for a while and then start the cooling process (unsynchronized cooling). In short, this kind of cooling prevents the battery from overcooling because the delay allows the battery to reach a higher temperature [39].

Liang et al. [39] found that cooling strategies with a lag time between the start-up of the HP-BTMS and the battery could enhance performance. However, adjusting the lag time

was difficult because it depended on the heat generation rate. The researchers suggested the use of a temperature difference between the inlet coolant temperature and the T_{max} (T_{bf}) because these temperatures were determinable. The T_{bf} was applied to control the start-up time. The T_{bf} determined the start-up of the BTMS, but it also depended on the T_{ab}. At T_{ab} = 15 °C, the BTMS could be started at T_{bf} = 15 °C. However, at T_{ab} = 25 °C, the BTMS could be started at T_{bf} = 10 °C.

Therefore, controlling the start-up time could help conserve power to turn on either the fan or the pump. Wan [59] studied the effects of the BTMS's start-up time and obtained the same results as Liang et al. [39].

2.6. Effects of the Inclination Angle of the Heat Pipe

The angle between the horizontal plane and the vertical axis (inclination angle) has a significant effect on the performance of a heat pipe [60].

Ye et al. [10] studied the effects of the orientation of the condensation section in three configurations: (1) the condenser on top and the evaporator on the bottom, (2) horizontal, and (3) the condenser on the bottom and the evaporator on top. Their results showed that the optimal performance was obtained when the condenser was on top.

Behi et al. [61] examined the inclination angle's effects on the performance of heat pipe-based air cooling for a lithium-titanate-oxide (LTO) cell by measuring the thermal resistance. They found that the temperature on the backside of the LTO cell and the heat pipe's thermal resistance decreased as the inclination angle increased (0° to 90°). In addition, it was obvious that the temperature difference between the condenser and evaporator sections decreased (from 5.26 to 5.04 °C) as the inclination angle increased (0° to 90°). The condensed water could return faster to the evaporator due to gravity.

Yao et al. [48] analyzed the effect of a heat pipe's tilt angle. They conducted the experiment under a heat generation of 10 W with natural air convection for tilt angles of −75°, −30°, 0°, 15°, 45°, and 90°. At a tilt angle of 90°, the T_{max} and ΔT were 60 and 3 °C, respectively. When the tilt angle was −75°, the T_{max} and ΔT increased to 88 and 16 °C, respectively. The authors showed that the effective thermal conductivity decreased with decreases in the tilt angles; for example, the effective thermal conductivity was 5820 $W \cdot m^{-1} \cdot K^{-1}$ at 90° and 295 $W \cdot m^{-1} \cdot K^{-1}$ at −75° [48].

In summary, the performance obtained from an HP-BTMS depends on the orientation angle of the unit. An increase in the inclination angle caused the condensed working fluid in the heat pipe to return to the evaporation section faster, which resulted in less flow resistance [61].

2.7. Effects of the Condenser and Evaporator Section Lengths

The heat pipe's total thermal resistance is the sum of the thermal resistance of the evaporator (R_e), adiabatic (R_a), and condenser (R_c), which can be expressed as

$$R_{hp} = R_e + R_a + R_c, \tag{3}$$

For the evaporator section, the thermal resistance is calculated as

$$R_e = \frac{1}{h_e A_e} \cong \frac{\delta}{k_l A_e}, \tag{4}$$

where h_e, δ, A_e, and k_l are the evaporation heat transfer coefficient, liquid film thickness, heating area, and thermal conductivity of the liquid, respectively [44]. The equation shows that the evaporator's thermal resistance is inversely proportional to its heating area (A_e), which is related to the heating length.

Nasir et al. [40] studied the effects of the condenser and evaporator sections' lengths on the performance of a heat pipe. Condenser section lengths of 100 and 150 mm were studied. A slight decrease and an uneven distribution of the battery's surface temperature were found. The authors also found that the surface temperature decreased in the range

of 0.949–2.96%. When the condenser section's length increased, the amount of condensed liquid would increase. This condensed liquid would be transported to the evaporator section and turned into vapors in the evaporator section. This implied more heat would be absorbed from the battery's surface; therefore, the battery's surface temperature decreased [40].

Nevertheless, the decrease in the T_{max}, (1.76%) was small. Moreover, with the increase in condenser length, the ΔT on the battery's surface increased moderately, from 0.142 to 5.34%. The researchers also observed a large drop in the total thermal resistance, which decreased by 5.12%. Moreover, the Nusselt number increased from 224 to 400 and from 205 to 319 when the battery heat generation rates were 10 and 15 W, respectively. The average increase was 45.1% when the condenser length increased by 50 mm, which implied that the condenser length had a vital effect on convective heat transfer to the condenser's external side.

Gan et al. [41] investigated the condenser length's effects on a BTMS's cooling performance. When the condenser length was increased from 6 to 42 mm, the T_{max} and ΔT decreased by 6.97 and 0.79 °C, respectively, as shown in Figure 12. Although the heat transfer area increased with an increased condenser length, an increase in length might cause the HP-BTMS's weight to increase. Therefore, selecting the appropriate condenser length enhances the BTMS's cooling performance.

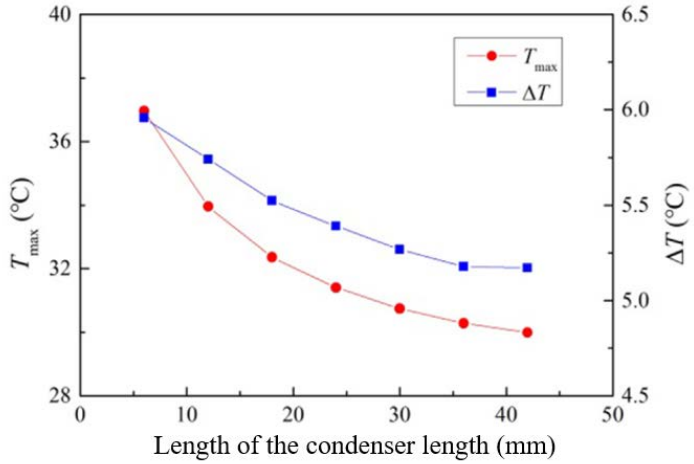

Figure 12. T_{max} and ΔT of the battery pack at a 2 C discharging rate with different condenser lengths (from Gan et al. [41], with permission from Elsevier).

We found that increasing either the condenser or evaporator length enhanced the thermal performance of a heat pipe. However, the length of either the evaporator or condenser section should be carefully investigated to avoid an increase in the HP-BTMS's weight and size.

3. Conclusions

In this paper, the effects of ambient temperature, coolant temperature, coolant flow rate, heat generation rate, start-up time, inclination angle of a heat pipe, and cooling/heating length on the performance of HP-BTMSs are reviewed. The results are useful for practical applications in the design of BTMSs.

Author Contributions: Writing—review and editing, K.B. and N.P.; writing—original draft preparation, H.M. Conceptualization, P.T., K.R. and Y.L.; review—editing and project administration, S.W. All authors have read and agreed to the published version of the manuscript.

Funding: The NSTDA Research Chair Grant, and the TSRI Fundamental Fund 2023.

Data Availability Statement: Not applicable.

Acknowledgments: The authors acknowledge NSTDA for the Research Chair Grant, and Thailand Science Research and Innovation (TSRI) for Fundamental Fund 2023.

Conflicts of Interest: The authors declare no conflict of interest.

References

1. Gou, J.; Liu, W. Feasibility study on a novel 3D vapor chamber used for Li-ion battery thermal management system of electric vehicle. *Appl. Therm. Eng.* **2019**, *152*, 362–369. [CrossRef]
2. Guo, S.; Xiong, R.; Wang, K.; Sun, F. A novel echelon internal heating strategy of cold batteries for all-climate electric vehicles application. *Appl. Energy* **2018**, *219*, 256–263. [CrossRef]
3. Rajan, A.; Vijayaraghavan, V.; Ooi, M.P.-L.; Garg, A.; Kuang, Y.C. A simulation-based probabilistic framework for lithium-ion battery modelling. *Measurement* **2018**, *115*, 87–94. [CrossRef]
4. Zhang, W.; Qiu, J.; Yin, X.; Wang, D. A novel heat pipe assisted separation type battery thermal management system based on phase change material. *Appl. Therm. Eng.* **2020**, *165*, 114571. [CrossRef]
5. Mbulu, H.; Laoonual, Y.; Wongwises, S. Experimental study on the thermal performance of a battery thermal management system using heat pipes. *Case Stud. Therm. Eng.* **2021**, *26*, 101029. [CrossRef]
6. Hu, Y.; Choe, S.; Garrick, T. Measurement of heat generation rate and heat sources of pouch type Li-ion cells. *Appl. Therm. Eng.* **2021**, *189*, 116709. [CrossRef]
7. Xu, J.; Lan, C.; Qiao, Y.; Ma, Y. Prevent thermal runaway of lithium-ion batteries with minichannel cooling. *Appl. Therm. Eng.* **2017**, *110*, 883–890. [CrossRef]
8. Jaguemont, J.; Boulon, L.; Dubé, Y. A comprehensive review of lithium-ion batteries used in hybrid and electric vehicles at cold temperatures. *Appl. Energy* **2016**, *164*, 99–114. [CrossRef]
9. Ye, Y.; Saw, L.H.; Shi, Y.; Tay, A.A. Numerical analyses on optimizing a heat pipe thermal management system for lithium-ion batteries during fast charging. *Appl. Therm. Eng.* **2015**, *86*, 281–291. [CrossRef]
10. Ye, Y.; Shi, Y.; Saw, L.H.; Tay, A.A. Performance assessment and optimization of a heat pipe thermal management system for fast charging lithium ion battery packs. *Int. J. Heat Mass Transf.* **2016**, *92*, 893–903. [CrossRef]
11. Pesaran, A.A. Battery thermal models for hybrid vehicle simulations. *J. Power Sources* **2002**, *110*, 377–382. [CrossRef]
12. Zhao, R.; Gu, J.; Liu, J. An experimental study of heat pipe thermal management system with wet cooling method for lithium ion batteries. *J. Power Sources* **2015**, *273*, 1089–1097. [CrossRef]
13. Hwang, H.-Y.; Chen, Y.-S.; Chen, J.-S. Optimizing the heat dissipation of an electric vehicle battery pack. *Adv. Mech. Eng.* **2015**, *7*, 204131. [CrossRef]
14. Chombo, P.V.; Laoonual, Y. A review of safety strategies of a Li-ion battery. *J. Power Sources* **2020**, *478*, 228649. [CrossRef]
15. Roe, C.; Feng, X.; White, G.; Li, R.; Wang, H.; Rui, X.; Li, C.; Zhang, F.; Null, V.; Parkes, M.; et al. Immersion cooling for lithium-ion batteries-A review. *J. Power Sources* **2022**, *525*, 231094.
16. Dan, D.; Yao, C.; Zhang, Y.; Zhang, H.; Zeng, Z.; Xu, X. Dynamic thermal behavior of micro heat pipe array-air cooling battery thermal management system based on thermal network model. *Appl. Therm. Eng.* **2019**, *162*, 114183. [CrossRef]
17. Yang, W.; Zhou, F.; Zhou, H.; Wang, Q.; Kong, J. Thermal performance of cylindrical lithium-ion battery thermal management system integrated with mini-channel liquid cooling and air cooling. *Appl. Therm. Eng.* **2020**, *175*, 115331.
18. Mahamud, R.; Park, C. Reciprocating air flow for Li-ion battery thermal management to improve temperature uniformity. *J. Power Sources* **2011**, *196*, 5685–5696. [CrossRef]
19. Park, H. A design of air flow configuration for cooling lithium ion battery in hybrid electric vehicles. *J. Power Sources* **2013**, *239*, 30–36.
20. Yang, W.; Zhou, F.; Zhou, H.; Liu, Y. Thermal performance of axial air cooling system with bionic surface structure for cylindrical lithium-ion battery module. *Int. J. Heat Mass Transf.* **2020**, *161*, 120307.
21. Buidin, T.I.C.; Mariasiu, F. Battery thermal management systems: Current status and design approach of cooling technologies. *Energies* **2021**, *14*, 4879. [CrossRef]
22. Wu, W.; Wang, S.; Wu, W.; Chen, K.; Hong, S.; Lai, Y. A critical review of battery thermal performance and liquid based battery thermal management. *Energy Convers. Manag.* **2019**, *182*, 262–281. [CrossRef]
23. Lai, Y.; Wu, W.; Chen, K.; Wang, S.; Xin, C. A compact and lightweight liquid-cooled thermal management solution for cylindrical lithium-ion power battery pack. *Int. J. Heat Mass Transf.* **2019**, *144*, 118581.
24. Murali, G.; Sravya, G.S.N.; Jaya, J.; Vamsi, V.N. A review on hybrid thermal management of battery packs and it's cooling performance by enhanced PCM. *Renew. Sustain. Energy Rev.* **2021**, *150*, 111513.
25. Singh, R.; Sadeghi, S.; Shabani, B. Thermal conductivity enhancement of phase change materials for low-temperature thermal energy storage applications. *Energies* **2019**, *12*, 75. [CrossRef]
26. Ping, P.; Peng, R.; Kong, D.; Chen, G.; Wen, J. Investigation on thermal management performance of PCM-fin structure for Li-ion battery module in high-temperature environment. *Energy Convers. Manag.* **2018**, *176*, 131–146.
27. Wu, W.; Yang, X.; Zhang, G.; Ke, X.; Wang, Z.; Situ, W.; Li, X.; Zhang, J. An experimental study of thermal management system using copper mesh-enhanced composite phase change materials for power battery pack. *Energy* **2016**, *113*, 909–916.

28. Zhang, C.W.; Chen, S.R.; Gao, H.B.; Xu, K.J.; Xia, Z.; Li, S.T. Study of thermal management system using composite phase change materials and thermoelectric cooling sheet for power battery pack. *Energies* **2019**, *12*, 1937. [CrossRef]
29. Zohuri, B. *Heat Pipe Design and Technology Modern Applications for Practical Thermal Management*, 2nd ed.; Springer: Cham, Switzerland, 2016.
30. Behi, H.; Ghanbarpour, M.; Behi, M. Investigation of PCM-assisted heat pipe for electronic cooling. *Appl. Therm. Eng.* **2017**, *127*, 1132–1142. [CrossRef]
31. Wu, M.-S.; Liu, K.; Wang, Y.-Y.; Wan, C.-C. Heat dissipation design for lithium-ion batteries. *J. Power Sources* **2002**, *109*, 160–166. [CrossRef]
32. Lei, S.; Shi, Y.; Chen, G. Heat-pipe based spray-cooling thermal management system for lithium-ion battery: Experimental study and optimization. *Int. J. Heat Mass Transf.* **2020**, *163*, 120494.
33. E, J.; Yi, F.; Li, W.; Zhang, B.; Zuo, H.; Wei, K.; Chen, J.; Zhu, H.; Zhu, H.; Deng, Y. Effect analysis on heat dissipation performance enhancement of a lithium-ion-battery pack with heat pipe for central and southern regions in China. *Energy* **2021**, *226*, 120336. [CrossRef]
34. Xu, X.; Tang, W.; Fu, J.; Li, R.; Sun, X. Plate flat heat pipe and liquid-cooled coupled multistage heat dissipation system of Li-ion battery. *Int. J. Energy Res.* **2018**, *43*, 1133–1141. [CrossRef]
35. Wang, Y.; Dan, D.; Xie, Y.; Li, W.; Guo, H.; Zhang, Y. Study on the influence of flat heat pipe structural parameters in battery thermal management system. *Front. Energy Res.* **2022**, *9*, 797664.
36. Wang, Y.; Dan, D.; Zhang, Y.; Qian, Y.; Panchal, S.; Fowler, M.; Li, W.; Tran, M.; Xie, Y. A novel heat dissipation based on flat heat pipe for battery thermal management system. *Int. J. Energy Res.* **2022**, *46*, 15961–15980. [CrossRef]
37. Huang, Q.; Li, X.; Zhang, G.; Zhang, J.; He, F.; Li, Y. Experimental investigation of the thermal performance of heat pipe pipe assisted phase change material for battery thermal management system. *Appl. Therm. Eng.* **2018**, *141*, 1092–1100.
38. Boonma, K.; Mesgarpour, M.; NajmAbad, J.M.; Alizadeh, R.; Mahian, O.; Dalkılıç, A.S.; Ahn, H.S.; Wongwises, S. Prediction of battery thermal behaviour in the presence of a constructal theory-based heat pipe (CBHP): A multiphysics model and pattern-based machine learning approach. *J. Energy Storage* **2022**, *48*, 103963.
39. Liang, J.; Gan, Y.; Li, Y. Investigation on the thermal performance of a battery thermal management system using heat pipe under different ambient temperatures. *Energy Convers. Manag.* **2018**, *155*, 1–9.
40. Nasir, F.M.; Abdullah, M.Z.; Ismail, M.A. Experimental investigation of water-cooled heat pipes in the thermal management of lithium-ion EV batteries. *Arab. J. Sci. Eng.* **2019**, *44*, 7541–7552.
41. Gan, Y.; He, L.; Liang, J.; Tan, M.; Xiong, T.; Li, Y. A numerical study on the performance of a thermal management system for a battery pack with cylindrical cells based on heat pipes. *Appl. Therm. Eng.* **2020**, *179*, 115740.
42. Zhang, Z.; Wei, K. Experimental and numerical study of a passive thermal management system using flat heat pipes for lithium-ion batteries. *Appl. Therm. Eng.* **2020**, *166*, 114660.
43. Zeng, W.; Niu, Y.; Li, S.; Hu, S.; Mao, B.; Zhang, Y. Cooling performance and optimization of a new hybrid thermal management system of cylindrical battery. *Appl. Therm. Eng.* **2022**, *217*, 119171.
44. Chien, L.-H.; Shih, Y.-C. An experimental study of mesh type flat heat pipes. *J. Mech.* **2011**, *27*, 167–176.
45. Rao, Z.; Wang, S.; Wu, M.; Lin, Z.; Li, F. Experimental investigation on thermal management of electric vehicle battery with heat pipe. *Energy Convers. Manag.* **2013**, *65*, 92–97.
46. Wang, Q.; Jiang, B.; Xue, Q.; Sun, H.; Li, B.; Zou, H.; Yan, Y. Experimental investigation on EV battery cooling and heating by heat pipes. *Appl. Therm. Eng.* **2015**, *88*, 54–60. [CrossRef]
47. Khateeb, S.A.; Amiruddin, S.; Farid, M.; Selman, J.R.; Al-Hallaj, S. Thermal management of Li-ion battery with phase change material for electric scooters: Experimental validation. *J. Power Sources* **2005**, *142*, 345–353.
48. Yao, C.; Dan, D.; Zhang, Y.; Wang, Y.; Qian, Y.; Yan, Y.; Zhuge, W. Thermal Performance of a Micro Heat Pipe Array for Battery Thermal Management Under Special Vehicle-Operating Conditions. *Automot. Innov.* **2020**, *3*, 317–327.
49. Wang, J.; Gan, Y.; Liang, J.; Tan, M.; Li, Y. Sensitivity analysis of factors influencing a heat pipe-based thermal management system for a battery module with cylindrical cells. *Appl. Therm. Eng.* **2019**, *151*, 475–485.
50. Chen, M.; Li, J. Nanofluid-based pulsating heat pipe for thermal management of lithium-ion batteries for electric vehicles. *J. Energy Storage* **2020**, *32*, 101715.
51. Jouhara, H.; Serey, N.; Khordehgah, N.; Bennett, R.; Almahmoud, S.; Lester, S.P. Investigation, development and experimental analyses of a heat pipe based battery thermal management system. *Int. J.* **2020**, *1*, 100004.
52. Behi, H.; Karimi, D.; Behi, M.; Ghanbarpour, M.; Jaguemont, J.; Sokkeh, M.A.; Gandoman, F.H.; Berecibar, M.; van Mierlo, J. A new concept of thermal management system in Li-ion battery using Fair cooling and heat pipe for electric vehicles. *Appl. Therm. Eng.* **2020**, *174*, 115280.
53. Alihosseini, A.; Shafaee, M. Experimental study and numerical simulation of a Lithium-ion battery thermal management system using a heat pipe. *J. Energy Storage* **2021**, *39*, 102616. [CrossRef]
54. Li, Y.; Guo, H.; Qi, F.; Guo, Z.; Li, M.; Tjernberg, L.B. Investigation on liquid cold plate thermal management system with heat pipes for LiFePO4 battery pack in electric vehicles. *Appl. Therm. Eng.* **2021**, *185*, 116382.
55. Behi, H.; Karimi, D.; Behi, M.; Jaguemont, J.; Ghanbarpour, M.; Behnia, M.; Berecibar, M.; Mierlo, J.V. Thermal management analysis using heat pipe in the high current discharging of lithium-ion battery in electric vehicles. *J. Energy Storage* **2020**, *32*, 101893. [CrossRef]

56. Wu, W.; Yang, X.; Zhang, G.; Chen, K.; Wang, S. Experimental investigation on the thermal performance of heat pipe-assisted phase change material based battery thermal management system. *Energy Convers. Manag.* **2017**, *138*, 486–492.
57. Wan, C. A Numerical Investigation of the Thermal Performances of an Array of Heat Pipes for Battery Thermal Management. *Fluid Dyn. Mater. Processing* **2019**, *15*, 343–356. [CrossRef]
58. Wan, C. Prediction on Transient Thermal Performance of Heat Pipe Array for a Battery Thermal Management. *Acad. J. Eng. Technol. Sci.* **2020**, *3*, 199–208.
59. Wan, C. Effect of Start-Up Time and Cycle Characteristic of Heat Pipe Array for a Battery Thermal Management. *Acad. J. Eng. Technol. Sci.* **2020**, *3*, 121–130.
60. Wu, Y.; Zhang, Z.; Li, W.; Xu, D. Effect of the inclination angle on the steady-state heat transfer performance of a thermosyphon. *Appl. Sci.* **2019**, *9*, 3324. [CrossRef]
61. Behi, H.; Karimi, D.; Jaguemont, J.; Berecibar, M.; van Mierlo, J. Experimental study on cooling performance of flat heat pipe for lithium-ion battery at various inclination angels. *Energy Perspect.* **2020**, *1*, 77–92.